mathematics

MDPI

Article

A Markov Chain Model for Approximating the Run Length Distributions of Poisson EWMA Charts under Linear Drifts

Honghao Zhao *, Huajun Tang, Chuan Pang and Huimin Jiang

Department of Decision Sciences, School of Business, Macau University of Science and Technology, Macau 999078, China
* Correspondence: hhzhao@must.edu.mo

Abstract: In addition to monitoring the Poisson mean rate with step shifts, increasing attention has been given to monitoring Poisson processes subject to linear trends. The exponentially weighted moving average (EWMA) control chart has been widely implemented to monitor normal processes, but it lacks investigation for detecting the Poisson mean change under a linear trend. In this paper, we analyze the performance of the EWMA chart by extending the Markov chain model from monitoring Poisson processes under a step shift to a Poisson process with linear drift. The results demonstrate that the proposed method is able to provide accurate average run length approximation, compared with the Monte Carlo simulation. Optimal design tables and sensitivity analysis are presented to facilitate the use of the EWMA chart in practice.

Keywords: average run length; exponentially weighted moving average; linear trend; poisson process

MSC: 62P30

Citation: Zhao, H.; Tang, H.; Pang, C.; Jiang, H. A Markov Chain Model for Approximating the Run Length Distributions of Poisson EWMA Charts under Linear Drifts. *Mathematics* **2022**, *10*, 4786. https://doi.org/10.3390/math10244786

Academic Editor: Christophe Chesneau

Received: 15 November 2022
Accepted: 13 December 2022
Published: 16 December 2022

1. Introduction

Recently, considerable attention has been paid to monitoring a sequence of count data, due to its wide applications in quality control in manufacturing processes, health surveillance in healthcare management and other applications [1–6]. In practice, the count data in a specific region or within a specific time period is often assumed to follow the Poisson distribution. For example, the number of nonconformities in a product, the patient arrivals in one day, and the number of disease cases reported in one year.

To detect the change in the Poisson distribution, many methods have been proposed. A simple charting method is the Shewhart control chart, which makes use of the current observation. To incorporate the effect of past observations, the cumulative sum (CUSUM) and exponentially weighted moving average (EWMA) charts have been developed. Both charts have been widely used and discussed in the literature due to their promising detection ability. Some pioneer studies for monitoring the Poisson mean using the CUSUM and EWMA chart include [7–10]. Furthermore, some recent research results include [11–23].

The above studies are very appealing, but their results are restricted by their assumptions. Actually, nearly all of the above research results are based on the common assumption on the shift pattern of the process mean. In particular, they assume a step shift in the Poisson mean, meaning that the process mean remains the same in its in-control state and moves to a constant new level when the shift occurs. In practice, other types of shift patterns may exist. Therefore, linear drifts, as one of the common mean shift pattern other than step shifts, are worthy of research and investigation due to their occurrence in practice. For example, in the industrial quality control, tool wear is usually a gradual process and may cause the increase in the number of nonconformities in a product. In this sense, the mean number of nonconformities may continue to increase due to the gradual tool wear process. In public health surveillance, with the outbreak of an infectious disease, apparently the number of daily new infected cases in a specific region will increase gradually. However, very little

attention has been given to the detection of changes in the Poisson mean rate with linear drifts, except for in [24,25]. However, they only compared the performance of the change point estimators under a linear drift, and monitoring the Poisson mean rate under linear drifts is not covered in their research.

To incorporate the Poisson mean under the linear trend issue, one can definitely modify the CUSUM-type control charts with step shift, and apply the modified CUSUM-type control charts to monitor the linear drifts in the Poisson process mean. Alternatively, the generalized likelihood ratio chart is another option to address linear drifts in the Poisson process mean, by estimating the change time using the maximum likelihood principle [26]. Furthermore, the EWMA chart can also be designed to detect the drifts in the Poisson mean rate. For the sake of simplicity, we investigate the detection ability of the EWMA chart in this research.

Note that the EWMA chart can be designed for a one-sided or two-sided form, according to its potential applications. In industry quality control and public health surveillance, an increase in the Poisson rate often indicates an increase in the nonconformities in a product or an increase in the incidence rate of a disease, respectively. On the other hand, a decrease in the Poisson mean implies an improvement of the corresponding systems. Thus, the detection of one-sided change is often crucial. Unlike the widely used one-sided Poisson CUSUM chart, the one-sided Poisson EWMA control chart lacks research, except for in [27].

In this paper, we investigate the performance of the one-sided Poisson EWMA control chart for monitoring linear drifts in the Poisson rate, by using Markov chain models. The rest of this paper is organized as follows. In Section 2, the one-sided Poisson EWMA chart based on transformations is presented. In Section 3, we provide the calculation based on the Markov chain model for both zero-state and steady-state average run length and investigate the approximation accuracy of the proposed methods. In Section 4, the design of a one-sided Poisson EWMA chart is discussed. In Section 5, a numeric example is demonstrated to illustrate the use of the proposed one-sided EWMA chart. In Section 6, a concluding remark is presented.

2. One-Sided Poisson EWMA Chart

Assume there exists a sequence of count observations, denoted as $X_1, X_{2,}\ldots$ These observations are independent and follow Poisson distribution with a mean of μ_t. When the process is in-control, the process mean is assumed to be known a priori, which is given by $\mu_t = \mu_0$. At an unknown time τ, the process becomes out-of-control, and its mean increases linearly at the rate of θ. The detailed expression is given by,

$$\mu_t = \begin{cases} \mu_0 > 0 & t \leq \tau - 1 \\ \mu_0 + (t - \tau + 1)\theta & t \geq \tau, \end{cases} \tag{1}$$

where θ is the drift size, and in this research we consider $\theta > 0$ only. The traditional Poisson EWMA statistic follows,

$$Q_t = \lambda X_t + (1 - \lambda)Q_{t-1}, \tag{2}$$

where λ is the smoothing parameter, which is between 0 and 1, and $Q_0 = \mu_0$. The asymptotic control limits for the two-sided cases are given by,

$$\begin{aligned} LCL &= \max\left\{0, \mu_0 - L\sqrt{\frac{\lambda}{2-\lambda}\mu}\right\} \\ UCL &= \mu_0 + L\sqrt{\frac{\lambda}{2-\lambda}\mu} \end{aligned} \tag{3}$$

For the purpose of the quick detection of a one-sided drift, one may consider to reset the EWMA statistics to μ_0 whenever it is smaller than μ_0 [27–30]. Then, the upper Poisson EWMA chart follows,

$$E_t^X = \max\left\{\mu_0, \lambda X_t + (1-\lambda)E_{t-1}^X\right\}, \tag{4}$$

where $E_0^X = \mu_0$, and it signals when E_t^X exceeds its control limit $h_X = \mu_0 + L\sqrt{\frac{\lambda}{2-\lambda}\mu}$.

Note that the Poisson distribution is asymmetric, and one may transform the observations to obtain a better normality. A simple way is to use the linear transformation [27], which is given by,

$$Y_t = \frac{X_t - \mu_o}{\sqrt{\mu_0}}, \tag{5}$$

where Y_t is asymptotically normal with mean 0 and variance 1. Then, the upper Poisson EWMA based on the transformed data becomes,

$$E_t^Y = \max\left\{0, \lambda Y_t + (1-\lambda)E_{t-1}^Y\right\}, \tag{6}$$

where $E_0^Y = 0$, and it signals when E_t^Y exceeds its control limits $h_Y = L\sqrt{\frac{\lambda}{2-\lambda}}$. Note that different EWMA schemes can be formulated by applying different resetting rules or different transformations (see examples in [22,31–35]). For the sake of simplicity, we only investigate the EWMA chart in Equation (6) in our study.

3. Calculation of *ARL* and Approximation Accuracy

To evaluate the detection ability of a control chart, it is common to maintain its level of false alarm, and then calculate its detection delay. A smaller value of detection delay indicates a better performance of the corresponding control chart. A common measure of the false alarm is the in-control ARL, which computes the expected number of observations until a signal is generated, given no change occurring, denoted as $ARL_0 = E(t_A|\tau = \infty)$. t_A is the time when a control chart alarms and τ is the change time. $\tau = \infty$ indicates that no change occurs. Based on the definition of ARL_0, the detection delay is often defined as $ARL_1 = E(t_A|\tau = 1)$, which measures the expected number of observations until a signal is generated, given that the change of the process mean occurs at the initial start-up of the control chart. This measure is also called zero-state ARL ($ZSARL$). Furthermore, the change in the process mean could take place at a later time rather than the initial time step. In such scenarios, the steady-state ARL, defined as $ARL_{SS} = \lim_{\tau\to\infty} E[t_A - \tau|t_A \geq \tau]$, is often used to describe the steady state performance of a control chart.

3.1. Calculation of Zero-State and Steady-State ARL

To compute the values of ARL_0 and ARL_1, various approaches have been proposed, such as the Monte Carlo simulation and integral equation approaches. Furthermore, the Markov chain model is another effective method to approximately compute ARL [8]. In the following, we present the ARL calculation of the proposed EWMA chart based on the Markov chain model.

By dividing the in-control region $[0, h_Y]$ of the proposed EWMA charting statistic into m subregions, labeled as $i = 1, 2, \ldots, m$, the width of each subregion becomes $w = 2h_Y/(2m-1)$ except for the first one with width $w/2$. Denote $P_t(i,j)$ as the transition probability of E_t^Y from state i to state j at time t. Then, the calculation of $P_t(i,j)$ is given by,

$$\begin{cases} P_t(i,j) = Pr\{E_t^Y in\ state\ j \mid E_t^Y in\ state\ i\} \\ \qquad = Pr\{(j-1)w - 0.5w < \lambda Y_t + (1-\lambda)(i-1)w \le (j-1)w + 0.5w\} \\ \qquad = Pr\left\{\dfrac{[j-1.5-(1-\lambda)(i-1)]w}{\lambda} < Y_t \le \dfrac{[j-0.5-(1-\lambda)(i-1)]w}{\lambda}\right\} \\ \qquad = F(c_2,\mu_t) - F(c_1,\mu_t), \qquad (i=1,2,\ldots,m, j \ne 1) \\ P_t(i,j) = Pr\{Y_t \le c_2\} = F(c_2,\mu_t), \qquad (i=1,2,\ldots,m, j=1) \end{cases} \tag{7}$$

where $c_1 = \frac{[j-1.5-(1-\lambda)(i-1)]w}{\lambda}\sqrt{\mu_0} + \mu_0$ and $c_2 = \frac{[j-0.5-(1-\lambda)(i-1)]w}{\lambda}\sqrt{\mu_0} + \mu_0$. $F(\cdot,\mu_t)$ is the cumulative distribution function of a Poisson-distributed random variable with mean μ_t.

According to [8], the probability transition matrix $\mathbf{R}_t$ is constructed by using $P_t(i,j)$ as its element in each row and column. When calculating the value of ARL_0, the process mean μ_0 does not change. Thus, the probability transition matrix $\mathbf{R}_t$ remains the same, denoted as $\mathbf{R}$, and the ARL_0 is computed by,

$$ARL_0 = \mathbf{p}_{ini}^T(\mathbf{I}-\mathbf{R})^{-1}\mathbf{1} \tag{8}$$

where $\mathbf{p}_{ini}$ is the initial probability vector corresponding to E_0^Y, and $\mathbf{1}$ is a column vector of ones [8].

When computing ARL_1, the process mean μ_t is time varying, so the probability transition matrix $\mathbf{R}_t$ changes over time. Then, the ARL is calculated by,

$$ARL_1 = \mathbf{p}_{ini}^T \sum_{t=1}^{\infty}(\prod_{s=0}^{t-1}\mathbf{R}_s\mathbf{1}), \tag{9}$$

where R_0 is the identity matrix [36]. Note that with the increase in μ_t, the charting statistic is becoming easier to signal. When the μ_t is large enough, the EWMA chart always signals within one step. In this sense, the probability transition matrix $\mathbf{R}_t$ becomes stabilized, denoted as $\mathbf{R}_\infty$. The time for $\mathbf{R}$ to stabilize is denoted as t_{max}. Then the formula for ARL_1 calculation follows,

$$ARL_1 = \mathbf{p}_{ini}^T\left\{\sum_{t=1}^{t_{max}-1}(\prod_{s=0}^{t-1}\mathbf{R}_s\mathbf{1}) + (\prod_{s=0}^{t_{max}}\mathbf{R}_s)(\mathbf{I}-\mathbf{R}_\infty)^{-1}\mathbf{1}\right\} \tag{10}$$

It is obvious that the ARL_1 has to be computed through iterations until time t reaches t_{max}. Instead of arbitrarily selecting a large value, we set a scheme to determine the value of t_{max}. At each time t, we calculate the value of $(\mathbf{I}-\mathbf{R})\mathbf{1}$ which measures the probability of reaching the out-of-control state. When the smallest element of $(\mathbf{I}-\mathbf{R})\mathbf{1}$ is larger than 0.9999, we believe the value of μ_t is large enough, indicating the transition matrix is stabilized. The corresponding time t is the t_{max} we used.

Based on the process for calculating ARL_1 through Equation (10), is it not complicated to obtain the equation for approximating the steady-state ARL. According to [37], the steady-state ARL can be obtained by replacing the initial probability vector $\mathbf{p}_{ini}$ in Equation (10) with the cyclical steady-state probability vector $\mathbf{p}_{ss}$. The vector $\mathbf{p}_{ss}$ can be calculated by solving the following system, which is given by,

$$\begin{aligned} & p = P^T p \\ \mathbf{s.t.} \quad & P = \begin{pmatrix} \mathbf{R} & (\mathbf{I}-\mathbf{R})\mathbf{1} \\ 1\cdots 0 & 0 \end{pmatrix} \\ & \mathbf{1}^T p = 1 \end{aligned} \tag{11}$$

then the steady-state ARL can be approximated by the following,

$$ARL_{ss} = \mathbf{p}_{ss}^{T}\left\{\sum_{t=1}^{t_{max}-1}\left(\prod_{s=0}^{t-1}\mathbf{R}_s\mathbf{1}\right) + \left(\prod_{s=0}^{t_{max}}\mathbf{R}_s\right)(\mathbf{I}-\mathbf{R}_\infty)^{-1}\mathbf{1}\right\} \quad (12)$$

3.2. Approximation Accuracy

Note that the in-control ARL calculation does not need iterations, and the corresponding formula has been widely used, since it was proposed by [8]. Thus, we investigate the approximation accuracy of the ARL_1 calculation.

When using the Markov chain model, the value of state m is the most important parameter to specify. Table 1 presents the ARL_1 values, which are calculated by Markov chain model and Monte Carlo simulation. Furthermore, the standard errors of the ARL_1 values are also presented for the results obtained by the Monte Carlo simulation. The in-control mean is $\mu_0 = 4$, the smoothing parameter is $\lambda = 0.05$, and the ARL_0 is 200. The results obtained through the Monte Carlo simulation are based on 80,000 replicates. Compared with the results from the Monte Carlo simulation, the Markov chain model provides close results through all hypothetical drift sizes. A similar pattern could be found in the results of the steady-state ARL, which are presented in Table 2.

Table 1. Zero-state ARL values with different drift sizes when $\mu_0 = 4$, $\lambda = 0.05$ and $ARL_0 = 200$.

θ	**Methods**			
	Monte Carlo	**Markov Chain**		
	m **= 100**	m **= 200**	m **= 300**	
0.001	132.10 ± 0.47	131.59	132.13	132.02
0.010	55.65 ± 0.20	55.51	55.64	55.62
0.020	39.81 ± 0.14	39.72	39.80	39.79
0.050	25.02 ± 0.09	25.00	25.04	25.03
0.100	17.53 ± 0.06	17.52	17.55	17.55
0.200	12.31 ± 0.04	12.31	12.32	12.32
0.500	7.75 ± 0.03	7.75	7.75	7.75
1.000	5.47 ± 0.02	5.47	5.47	5.47

Table 2. Steady-state ARL values with different drift sizes when $\mu_0 = 4$, $\lambda = 0.05$ and $ARL_0 = 200$, given $\tau = 50$.

θ	**Methods**			
	Monte Carlo	**Markov Chain**		
	m **= 100**	m **= 200**	m **= 300**	
0.001	125.11 ± 0.33	125.64	125.75	125.63
0.010	52.80 ± 0.10	52.82	52.84	52.81
0.020	37.64 ± 0.06	37.67	37.68	37.67
0.050	23.42 ± 0.03	23.49	23.5	23.49
0.100	16.31 ± 0.02	16.3	16.3	16.3
0.200	11.28 ± 0.01	11.29	11.3	11.3
0.500	6.97 ± 0.007	6.97	6.97	6.97
1.000	4.86 ± 0.005	4.86	4.86	4.86

Furthermore, we can find that larger m produces better approximation. More specifically, when $m = 100$, the results obtained by the Markov chain model is very close to the values obtained by the Monte Carlo simulation, but still have very small differences. When $m = 200$ and 300, the approximation results become even better. However, a large value of m introduces the high computational load. Brook and Evans [8] suggested to use $m = 30$, and in our study we propose to select $m = 100$. It is important to reduce the computational load, since $m = 100$ already guarantees the approximation accuracy.

4. Design of the One-Sided Poisson EWMA Chart

The design of the EMWA chart is to determine the value of the two parameters, λ and L. According to [37], the design issue is to find the value of λ, which optimizes the detection ability for a specified drift in the Poisson mean rate, and select the value of L to produce the desired in-control ARL. Instead of theoretically calculating the optimal values of λ and L, extensive computation is implemented to search the optimal values of λ and L numerically. Tables 3–6 present a list of optimal λ and L pairs, which provide in-control ARL of 200, 500, 800 and 1000, respectively.

Table 3. Optimal parameters for the EWMA chart when $ARL_0 = 200$.

θ	μ_0			
	4	**8**	**12**	**16**
0.01				
(λ^*, L)	(0.04, 2.109)	(0.04, 2.094)	(0.03, 1.969)	(0.02, 1.777)
ARL_{min}	55.41	64.8	70.75	75.1
0.02				
(λ^*, L)	(0.05, 2.207)	(0.04, 2.094)	(0.04, 2.094)	(0.05, 2.172)
ARL_{min}	39.81	47.04	51.91	55.49
0.03				
(λ^*, L)	(0.07, 2.344)	(0.05, 2.184)	(0.05, 2.176)	(0.05, 2.172)
ARL_{min}	32.41	38.54	42.65	45.69
0.04				
(λ^*, L)	(0.07, 2.344)	(0.06, 2.262)	(0.06, 2.250)	(0.05, 2.172)
ARL_{min}	27.9	33.32	36.92	39.65
0.05				
(λ^*, L)	(0.09, 2.441)	(0.06, 2.262)	(0.07, 2.305)	(0.06, 2.250)
ARL_{min}	24.8	29.7	32.93	35.43
0.06				
(λ^*, L)	(0.09, 2.441)	(0.08, 2.371)	(0.07, 2.305)	(0.06, 2.250)
ARL_{min}	22.49	26.96	29.94	32.27
0.07				
(λ^*, L)	(0.10, 2.480)	(0.08, 2.371)	(0.07, 2.305)	(0.06, 2.250)
ARL_{min}	20.68	24.84	27.62	29.79
0.08				
(λ^*, L)	(0.10, 2.480)	(0.09, 2.406)	(0.09, 2.398)	(0.08, 2.346)
ARL_{min}	19.23	23.11	25.73	27.76
0.09				
(λ^*, L)	(0.12, 2.551)	(0.09, 2.406)	(0.09, 2.398)	(0.08, 2.346)
ARL_{min}	18.02	21.69	24.14	26.07
0.10				
(λ^*, L)	(0.12, 2.551)	(0.11, 2.480)	(0.09, 2.398)	(0.08, 2.346)
ARL_{min}	17	20.48	22.81	24.64
0.11				
(λ^*, L)	(0.12, 2.551)	(0.12, 2.512)	(0.09, 2.398)	(0.09, 2.391)
ARL_{min}	16.13	19.43	21.66	23.41
0.12				
(λ^*, L)	(0.12, 2.551)	(0.12, 2.512)	(0.11, 2.466)	(0.09, 2.391)
ARL_{min}	15.38	18.52	20.65	22.33
0.13				
(λ^*, L)	(0.15, 2.633)	(0.12, 2.512)	(0.11, 2.466)	(0.10, 2.430)
ARL_{min}	14.7	17.71	19.76	21.38
0.14				
(λ^*, L)	(0.16, 2.653)	(0.12, 2.512)	(0.11, 2.466)	(0.11, 2.453)
ARL_{min}	14.1	17	18.97	20.52
0.15				
(λ^*, L)	(0.16, 2.653)	(0.12, 2.512)	(0.11, 2.466)	(0.11, 2.453)
ARL_{min}	13.56	16.36	18.26	19.75
0.16				
(λ^*, L)	(0.16, 2.653)	(0.12, 2.512)	(0.12, 2.492)	(0.11, 2.453)
ARL_{min}	13.08	15.79	17.62	19.06
0.17				
(λ^*, L)	(0.16, 2.653)	(0.14, 2.555)	(0.12, 2.492)	(0.11, 2.453)
ARL_{min}	12.64	15.26	17.04	18.43
0.18				
(λ^*, L)	(0.16, 2.653)	(0.14, 2.555)	(0.12, 2.492)	(0.11, 2.453)
ARL_{min}	12.24	14.78	16.51	17.86
0.19				
(λ^*, L)	(0.16, 2.653)	(0.14, 2.555)	(0.12, 2.492)	(0.12, 2.484)
ARL_{min}	11.87	14.33	16.02	17.33
0.20				
(λ^*, L)	(0.18, 2.695)	(0.15, 2.584)	(0.12, 2.492)	(0.13, 2.508)
ARL_{min}	11.53	13.93	15.57	16.84

Table 4. Optimal parameters for the EWMA chart when $ARL_0 = 500$.

θ	μ_0			
	4	**8**	**12**	**16**
0.01				
(λ^*, L)	(0.03, 2.447)	(0.03, 2.434)	(0.02, 2.258)	(0.02, 2.252)
ARL_{min}	70.14	84.01	93	100.01
0.02				
(λ^*, L)	(0.04, 2.568)	(0.04, 2.541)	(0.03, 2.428)	(0.03, 2.418)
ARL_{min}	48.31	58.21	64.85	69.88
0.03				
(λ^*, L)	(0.05, 2.652)	(0.04, 2.541)	(0.04, 2.531)	(0.04, 2.526)
ARL_{min}	38.61	46.64	52.06	56.28
0.04				
(λ^*, L)	(0.06, 2.721)	(0.05, 2.627)	(0.05, 2.613)	(0.04, 2.526)
ARL_{min}	32.84	39.74	44.44	48.07
0.05				
(λ^*, L)	(0.07, 2.785)	(0.06, 2.689)	(0.05, 2.613)	(0.05, 2.605)
ARL_{min}	28.93	35.05	39.23	42.48
0.06				
(λ^*, L)	(0.08, 2.824)	(0.07, 2.748)	(0.06, 2.672)	(0.06, 2.666)
ARL_{min}	26.07	31.61	35.38	38.34
0.07				
(λ^*, L)	(0.09, 2.873)	(0.07, 2.748)	(0.06, 2.672)	(0.06, 2.666)
ARL_{min}	23.85	28.95	32.43	35.13
0.08				
(λ^*, L)	(0.09, 2.873)	(0.08, 2.787)	(0.07, 2.726)	(0.06, 2.666)
ARL_{min}	22.09	26.81	30.07	32.58
0.09				
(λ^*, L)	(0.10, 2.906)	(0.08, 2.787)	(0.08, 2.766)	(0.07, 2.715)
ARL_{min}	20.64	25.06	28.09	30.46
0.10				
(λ^*, L)	(0.11, 2.938)	(0.09, 2.827)	(0.08, 2.766)	(0.07, 2.715)
ARL_{min}	19.42	23.58	26.43	28.68
0.11				
(λ^*, L)	(0.11, 2.938)	(0.10, 2.863)	(0.08, 2.766)	(0.08, 2.762)
ARL_{min}	18.37	22.32	25.02	27.15
0.12				
(λ^*, L)	(0.11, 2.938)	(0.10, 2.863)	(0.09, 2.804)	(0.08, 2.762)
ARL_{min}	17.47	21.21	23.79	25.82
0.13				
(λ^*, L)	(0.13, 2.993)	(0.10, 2.863)	(0.10, 2.834)	(0.08, 2.762)
ARL_{min}	16.67	20.25	22.71	24.66
0.14				
(λ^*, L)	(0.13, 2.993)	(0.10, 2.863)	(0.10, 2.834)	(0.09, 2.795)
ARL_{min}	15.96	19.39	21.75	23.62
0.15				
(λ^*, L)	(0.14, 3.017)	(0.11, 2.887)	(0.10, 2.834)	(0.10, 2.828)
ARL_{min}	15.33	18.63	20.89	22.69
0.16				
(λ^*, L)	(0.14, 3.017)	(0.13, 2.936)	(0.10, 2.834)	(0.10, 2.828)
ARL_{min}	14.76	17.93	20.12	21.84
0.17				
(λ^*, L)	(0.14, 3.017)	(0.13, 2.936)	(0.11, 2.866)	(0.10, 2.828)
ARL_{min}	14.24	17.3	19.42	21.08
0.18				
(λ^*, L)	(0.15, 3.041)	(0.13, 2.936)	(0.11, 2.866)	(0.10, 2.828)
ARL_{min}	13.77	16.72	18.78	20.39
0.19				
(λ^*, L)	(0.15, 3.041)	(0.13, 2.936)	(0.12, 2.893)	(0.11, 2.853)
ARL_{min}	13.34	16.2	18.19	19.75
0.20				
(λ^*, L)	(0.15, 3.041)	(0.13, 2.936)	(0.12, 2.893)	(0.11, 2.853)
ARL_{min}	12.95	15.71	17.65	19.17

To demonstrate the use of these design tables and the process for calculating these tables, we present an example. Suppose that we are aiming to find the optimal values of λ and L for a target drift size $\theta = 0.01$ with in-control mean $\mu_0 = 4$ and in-control ARL $ARL_0 = 200$. We first create a wide range of λ with step size 0.01, for example, $\lambda = 0.01, 0.02, \ldots$ Then, we select the value of L for each λ to achieve $ARL_0 = 200$. Based on each pair of λ and L, the out-of-control ARL ARL_1 is computed. The pair of λ and L ($\lambda = 0.04, L = 2.109$), which produces the minimum value of ARL_1 ($ARL_{min} = 55.41$), becomes the optimal design for the above requirement.

Table 5. Optimal parameters for the EWMA chart when $ARL_0 = 800$.

θ	μ_0			
	4	**8**	**12**	**16**
0.01				
(λ^*, L)	(0.03, 2.674)	(0.02, 2.489)	(0.02, 2.479)	(0.02, 2.470)
ARL_{min}	76.75	92.54	103.11	111.35
0.02				
(λ^*, L)	(0.04, 2.783)	(0.03, 2.646)	(0.03, 2.636)	(0.03, 2.631)
ARL_{min}	52.19	63.16	70.63	76.47
0.03				
(λ^*, L)	(0.05, 2.857)	(0.04, 2.751)	(0.04, 2.736)	(0.04, 2.729)
ARL_{min}	41.35	50.3	56.29	61.01
0.04				
(λ^*, L)	(0.06, 2.924)	(0.05, 2.826)	(0.05, 2.814)	(0.04, 2.729)
ARL_{min}	35.03	42.6	47.79	51.78
0.05				
(λ^*, L)	(0.07, 2.980)	(0.06, 2.887)	(0.05, 2.814)	(0.05, 2.803)
ARL_{min}	30.78	37.45	42	45.58
0.06				
(λ^*, L)	(0.07, 2.980)	(0.06, 2.887)	(0.06, 2.873)	(0.05, 2.803)
ARL_{min}	27.68	33.68	37.81	41.02
0.07				
(λ^*, L)	(0.10, 3.098)	(0.07, 2.939)	(0.06, 2.873)	(0.06, 2.862)
ARL_{min}	25.26	30.78	34.56	37.53
0.08				
(λ^*, L)	(0.10, 3.098)	(0.07, 2.939)	(0.07, 2.920)	(0.06, 2.862)
ARL_{min}	23.33	28.47	31.98	34.71
0.09				
(λ^*, L)	(0.10, 3.098)	(0.08, 2.981)	(0.07, 2.920)	(0.07, 2.909)
ARL_{min}	21.75	26.56	29.84	32.41
0.10				
(λ^*, L)	(0.10, 3.098)	(0.08, 2.981)	(0.08, 2.959)	(0.07, 2.909)
ARL_{min}	20.43	24.96	28.05	30.46
0.11				
(λ^*, L)	(0.10, 3.098)	(0.09, 3.018)	(0.08, 2.959)	(0.07, 2.909)
ARL_{min}	19.32	23.6	26.51	28.81
0.12				
(λ^*, L)	(0.10, 3.098)	(0.09, 3.018)	(0.08, 2.959)	(0.08, 2.949)
ARL_{min}	18.36	22.42	25.19	27.36
0.13				
(λ^*, L)	(0.10, 3.098)	(0.09, 3.018)	(0.09, 2.994)	(0.08, 2.949)
ARL_{min}	17.52	21.39	24.02	26.1
0.14				
(λ^*, L)	(0.10, 3.098)	(0.11, 3.075)	(0.09, 2.994)	(0.08, 2.949)
ARL_{min}	16.79	20.47	22.99	24.98
0.15				
(λ^*, L)	(0.13, 3.189)	(0.11, 3.075)	(0.09, 2.994)	(0.09, 2.982)
ARL_{min}	16.12	19.64	22.07	23.99
0.16				
(λ^*, L)	(0.13, 3.189)	(0.11, 3.075)	(0.10, 3.025)	(0.09, 2.982)
ARL_{min}	15.51	18.9	21.24	23.08
0.17				
(λ^*, L)	(0.13, 3.189)	(0.11, 3.075)	(0.10, 3.025)	(0.09, 2.982)
ARL_{min}	14.96	18.23	20.49	22.27
0.18				
(λ^*, L)	(0.13, 3.189)	(0.12, 3.103)	(0.11, 3.050)	(0.09, 2.982)
ARL_{min}	14.46	17.62	19.8	21.53
0.19				
(λ^*, L)	(0.15, 3.235)	(0.12, 3.103)	(0.11, 3.050)	(0.09, 2.982)
ARL_{min}	14	17.06	19.17	20.86
0.20				
(λ^*, L)	(0.15, 3.235)	(0.13, 3.126)	(0.11, 3.050)	(0.11, 3.035)
ARL_{min}	13.58	16.55	18.59	20.24

Note that small values of λ are sensitive to small drifts, and large values of λ are sensitive to large drifts. Taking $ARL_0 = 200$ and $\mu_0 = 4$ as an example, the optimal λ for detecting drift $\theta = 0.01$ is 0.04, and the optimal λ for drift size $\theta = 0.20$ is 0.18. Furthermore, the optimal values of λ increase with the increase in drift size θ.

It is interesting to note that the in-control mean μ_0 affects the choice of optimal parameters. For a desired in-control ARL, the optimal value of λ decreases with the increase in μ_0. This trend is more obvious when the target drift size is large. Furthermore, there do exist exceptions. For example, the optimal value of λ is 0.12 for $\theta = 0.20$, $\mu_0 = 12$, and $ARL_0 = 200$. However, the optimal value of λ is 0.13 for $\theta = 0.20$, $\mu_0 = 16$, and

$ARL_0 = 200$. This phenomenon may result from the step size. If the step size is small enough, the optimal value of λ can be more accurate.

Table 6. Optimal parameters for the EWMA chart when $ARL_0 = 1000$.

θ	μ_0			
	4	**8**	**12**	**16**
0.01				
(λ^*, L)	(0.03, 2.763)	(0.02, 2.590)	(0.02, 2.581)	(0.02, 2.579)
ARL_{min}	79.69	96.31	107.57	116.37
0.02				
(λ^*, L)	(0.04, 2.875)	(0.03, 2.741)	(0.03, 2.731)	(0.03, 2.725)
ARL_{min}	53.78	65.31	73.17	79.35
0.03				
(λ^*, L)	(0.05, 2.951)	(0.04, 2.844)	(0.04, 2.838)	(0.03, 2.725)
ARL_{min}	42.57	51.81	58.08	63.05
0.04				
(λ^*, L)	(0.06, 3.025)	(0.05, 2.929)	(0.04, 2.838)	(0.04, 2.825)
ARL_{min}	36.03	43.82	49.2	53.42
0.05				
(λ^*, L)	(0.07, 3.074)	(0.05, 2.929)	(0.05, 2.906)	(0.05, 2.895)
ARL_{min}	31.62	38.48	43.23	46.97
0.06				
(λ^*, L)	(0.08, 3.122)	(0.07, 3.029)	(0.05, 2.906)	(0.05, 2.895)
ARL_{min}	28.39	34.64	38.87	42.21
0.07				
(λ^*, L)	(0.08, 3.122)	(0.07, 3.029)	(0.06, 2.961)	(0.05, 2.895)
ARL_{min}	25.9	31.6	35.5	38.59
0.08				
(λ^*, L)	(0.08, 3.122)	(0.07, 3.029)	(0.06, 2.961)	(0.06, 2.947)
ARL_{min}	23.94	29.2	32.83	35.67
0.09				
(λ^*, L)	(0.09, 3.161)	(0.08, 3.071)	(0.07, 3.010)	(0.06, 2.947)
ARL_{min}	22.34	27.24	30.61	33.28
0.10				
(λ^*, L)	(0.10, 3.198)	(0.10, 3.129)	(0.08, 3.042)	(0.07, 2.994)
ARL_{min}	20.98	25.57	28.74	31.27
0.11				
(λ^*, L)	(0.10, 3.198)	(0.10, 3.129)	(0.08, 3.042)	(0.07, 2.994)
ARL_{min}	19.83	24.13	27.14	29.55
0.12				
(λ^*, L)	(0.10, 3.198)	(0.10, 3.129)	(0.08, 3.042)	(0.08, 3.033)
ARL_{min}	18.83	22.9	25.77	28.07
0.13				
(λ^*, L)	(0.11, 3.224)	(0.10, 3.129)	(0.08, 3.042)	(0.08, 3.033)
ARL_{min}	17.96	21.82	24.58	26.76
0.14				
(λ^*, L)	(0.11, 3.224)	(0.10, 3.129)	(0.08, 3.042)	(0.08, 3.033)
ARL_{min}	17.18	20.87	23.53	25.6
0.15				
(λ^*, L)	(0.12, 3.252)	(0.10, 3.129)	(0.08, 3.042)	(0.09, 3.066)
ARL_{min}	16.49	20.03	22.59	24.57
0.16				
(λ^*, L)	(0.14, 3.302)	(0.10, 3.129)	(0.10, 3.110)	(0.10, 3.098)
ARL_{min}	15.86	19.28	21.74	23.63
0.17				
(λ^*, L)	(0.14, 3.302)	(0.10, 3.129)	(0.10, 3.110)	(0.10, 3.098)
ARL_{min}	15.29	18.6	20.96	22.78
0.18				
(λ^*, L)	(0.14, 3.302)	(0.10, 3.129)	(0.10, 3.110)	(0.10, 3.098)
ARL_{min}	14.77	17.98	20.26	22.01
0.19				
(λ^*, L)	(0.14, 3.302)	(0.10, 3.129)	(0.10, 3.110)	(0.10, 3.098)
ARL_{min}	14.3	17.42	19.61	21.3
0.20				
(λ^*, L)	(0.14, 3.302)	(0.10, 3.129)	(0.11, 3.138)	(0.10, 3.098)
ARL_{min}	13.87	16.9	19.02	20.66

5. A Simulated Example

To demonstrate the use of the one-sided Poisson EWMA chart, a simulated example studied by Perry [24] is discussed. Such an example could be an abstraction or expression on the practice of monitoring daily new infected cases in a hospital. In this example, there are totally 40 observations. The process is in-control for the first 25 observations, and becomes out-of-control from the 26th observation. Note that all observations are generated from

the Poisson distribution. In particular, for the in-control state, the process mean is set to 5 ($\mu_0 = 5$). The process mean for the out-of-control state is set to $\mu_t = \mu_0 + 0.15(t - 25)$ ($26 \leq t \leq 40$). It is not hard to observe that the process mean takes a linear drift time of 26.

To facilitate the EWMA chart, we need to specify the smoothing parameter λ and the control limit h_Y. Assume that the desired in-control ARL is 200. According to Table 3, the optimal parameters for detecting drift size $\theta = 0.15$ can be chosen as $\lambda = 0.15$ and $h_Y = L\sqrt{\frac{\lambda}{2-\lambda}} = 0.7454$ by interpolation. Figure 1 presents the simulated counts and the charting statistics. The EWMA signals at time index 37.

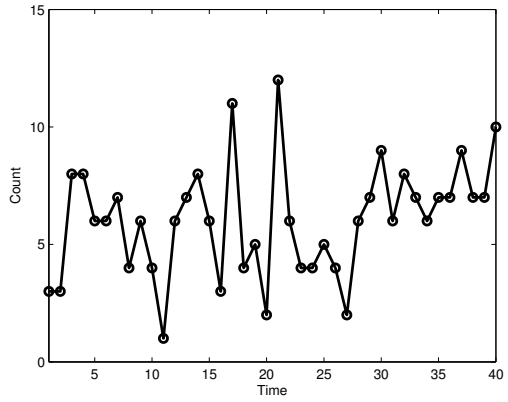

(**a**) Simulated Counts

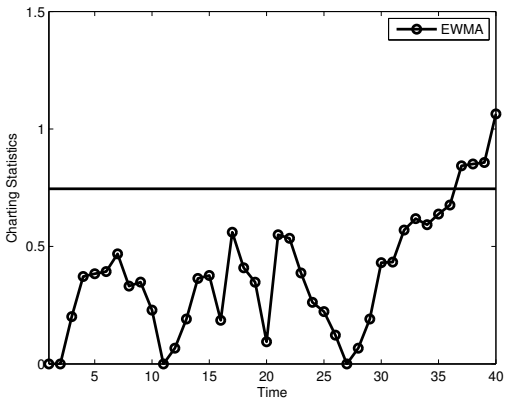

(**b**) Scaled Statistics

Figure 1. Simulated count data and the charting statistics.

6. Concluding Remarks

In this research, we analyze the detection ability of the one-sided Poisson EWMA chart for monitoring the Poisson mean subject to linear drifts. We apply the Markov chain model to evaluate the performance of the EWMA chart by extending it from step shifts to linear drifts. The results obtained from the Markov chain model are compared with the results generated by the Monte Carlo simulation. The comparison results demonstrated that the extended Markov chain model can produce accurate approximation. Some design tables are presented to facilitate the design of the one-sided Poisson EWMA chart.

In this work, only one type of the EMWA chart has been discussed. One can definitely investigate the performance of other EWMA charts, and even compare their performance when the Poisson mean performs a linear trend. Furthermore, we limited our studies to linear drifts. Other mean shift types can be considered, and our method can be adjusted to the other shift type easily, unless the shift pattern is known or can be estimated.

We assume that the in-control mean μ_0 is known in this work. However, it is reasonable that the in-control mean is unknown. As we discussed previously, the in-control mean

impacts the optimal value of the parameters. Thus, the precise estimation of the in-control mean μ_0 becomes crucial. It could be interesting to incorporate the uncertainty of the in-control mean, which is our further research.

Author Contributions: Conceptualization, H.Z.; methodology, H.Z.; validation, H.T.; writing—original draft preparation, H.Z.; writing—review and editing, H.T. and C.P.; supervision, C.P.; funding acquisition, H.T. and H.J. All authors have read and agreed to the published version of the manuscript.

Funding: This research was funded by the National Natural Science Foundation of China (grant number 71901149).

Data Availability Statement: Not applicable.

Conflicts of Interest: The authors declare no conflict of interest.

References

1. Woodall, W.H. The Use of Control Charts in Health-Care and Public-Health Surveillance. *J. Qual. Technol.* **2006**, *38*, 1–16. [CrossRef]
2. Rolka, H.; Burkom, H.; Cooper, G.F.; Kulldorff, M.; Madigan, D.; Wong, W.K. Issues in Applied Statistics for Public Health Bioterrorism Surveillance Using Multiple Data Streams: Research Needs. *Stat. Med.* **2007**, *26*, 1834–1856. [CrossRef]
3. Shmueli, G.; Burkom, H.S. Statistical Challenges Facing Early Outbreak Detection in Biosurveillance. *Technometrics* **2010**, *52*, 39–51. [CrossRef]
4. Tsui, K.L.; Chiu, W.; Gierlich, P.; Goldsman, D.; Liu, X.; Maschek, T. A Review of Healthcare, Public Health, and Syndromic Surveillance. *Qual. Eng.* **2008**, *20*, 435–450. [CrossRef]
5. Tsui, K.L.; Wong, Z.; Jiang, W.; Lin, C.J. Recent Research and Development in Temporal and Spatiotemporal Surveillance for Public Health. *IEEE Trans. Reliab.* **2011**, *60*, 49–58. [CrossRef]
6. Tang, H.J.; Elalouf, A.; Levner, E.; Cheng, T.C.E. Efficient computation of evacuation routes on a three-dimensional geometric network. *Comput. Ind. Eng.* **2014**, *76*, 231–242. [CrossRef]
7. Page, E.S. Continuous Inspection Schemes. *Biometrika* **1954**, *41*, 100–115. [CrossRef]
8. Brook, D.; Evans, D.A. An Approach to the Probability Distribution of Run Length. *Biometrika* **1972**, *59*, 539–549. [CrossRef]
9. Lucas, J.M. Counted data CUSUM's. *Technometrics* **1985**, *27*, 129–144. [CrossRef]
10. Gan, F.F. Monitoring poisson observations using modified exponentially weighted moving average control charts. *Commun. Stat. Simul. Comput.* **1990**, *19*, 103–124. [CrossRef]
11. White, C.H.; Keats, J.B. ARLs and Higher-order Run-length Moments for the Poisson CUSUM. *J. Qual. Technol.* **1996**, *28*, 363–369. [CrossRef]
12. White, C.H.; Keats, J.B.; Stanley, J. Poisson CUSUM Versus c Chart for Defect Data. *Qual. Eng.* **1997**, *9*, 673–679. [CrossRef]
13. Hawkins, D.M.; Olwell, D.H. *Cumulative Sum Charts and Charting for Quality Improvement*; Springer: Berlin, Germany, 1998.
14. Chan, L.Y.; Ouyang, J.; Lau, H.Y.K. A Two-stage Cumulative Quantity Control Chart for Monitoring Poisson Processes. *J. Qual. Technol.* **2007**, *39*, 203–223. [CrossRef]
15. Han, S.W.; Tsui, K.L.; Ariyajunya, B.; Kim, S.B. A Comparison of CUSUM, EWMA, and Temporal Scan Statistics for Detection of Increases in Poisson Rates. *Qual. Reliab. Eng. Int.* **2010**, *26*, 279–289. [CrossRef]
16. Ryan, A.G.; Woodall, W.H. Control Charts for Poisson Count Data with Varying Sample Size. *J. Qual.* **2010**, *42*, 260–275. [CrossRef]
17. Aebtarm, S.; Bouguila, N. An Empirical Evaluation of Attribute Control Charts for Monitoring Defects. *Expert Syst. Appl.* **2011**, *38*: 7869–7880. [CrossRef]
18. Mei, Y.J.; Han, S.W.; Tsui, K.L. Early Detection of a Change in Poisson Rate after Accounting for Population Size Effects. *Stat. Sin.* **2011**, *21*, 597–624. [CrossRef]
19. Jiang, W.; Shu, L.J.; Tsui, K.L. Weighted CUSUM Control Charts for Monitoring Poisson Processes with Varying Sample Size. *J. Qual. Technol.* **2011**, *43*, 346–362. [CrossRef]
20. Martz, H.F.; Kvam, P.H. Detecting Trends and Patterns in Reliability Data over Time Using Exponentially Weighted Moving-averages. *Reliab. Eng. Syst. Saf.* **1996**, *51*, 201–207. [CrossRef]
21. Borror, C.M.; Champ, C.W.; Rigdon, S.E. Poisson EWMA control charts. *J. Qual. Technol.* **1998**, *30*, 352–361. [CrossRef]
22. Shu, L.J.; Jiang, W.; Tsui, K.L. A Comparison of Weighted CUSUM Procedures that Account for Monotone Changes in Population Size. *Stat. Med.* **2011**, *30*, 725–741. [CrossRef]
23. Zhao, H.; Shu, L.; Jiang, W.; Tsui, K.L. An adaptive CUSUM chart for monitoring poisson rates with increasing population sizes. *Eur. J. Ind. Eng.* **2015**, *9*, 692–715. [CrossRef]
24. Perry, M.B.; Pignatiello, J.J.; Simpson, J.R. Estimating the Change Point of a Poisson Rate Parameter with a Linear Trend Disturbance. *Qual. Reliab. Eng. Int.* **2006**, *22*, 371–384. [CrossRef]
25. Perry, M.B.; Pignatiello, J.J.; Simpson, J.R. Change Point Estimation for Monotonically Changing Poisson Rates in SPC. *Int. J. Prod. Res.* **2007**, *45*, 1791–1813. [CrossRef]

26. Zhao, H.; Shu, L.; Tsui, K.L. A window-limited generalized likelihood ratio test for monitoring Poisson processes with linear drifts. *J. Stat. Comput. Simul.* **2015**, *85*, 2975–2988. [CrossRef]
27. Shu, L.; Jiang, W.; Wu, Z. Exponentially Weighted Moving Average Control Charts for Monitoring Increases in Poisson Rate. *IIE Trans.* **2012**, *44*, 711–723. [CrossRef]
28. Champ, C.W.; Woodall, W.H.; Mohsen, H.A. A generalized quality control procedure. *Stat. Probab. Lett.* **1991**, *11*, 211–218. [CrossRef]
29. Crowder, S.V.; Hamilton, M. Average run lengths of EWMA controls for monitoring a process standard deviation. *J. Qual. Technol.* **1992**, *24*, 44–50. [CrossRef]
30. Gan, F.F. Designs of one- and two-sided exponential EWMA charts. *J. Qual. Technol.* **1998**, *30*, 55–69. [CrossRef]
31. Quesenberry, C.P. SPC Q charts for start-up processes and short and long runs. *J. Qual. Technol.* **1991**, *23*, 213–224. [CrossRef]
32. Quesenberry, C.P. SPC Q charts for a binomial parameter: Short and long runs. *J. Qual. Technol.* **1991**, *23*, 239–246. [CrossRef]
33. Quesenberry, C.P. SPC Q charts for a Poisson parameter λ: Short and long runs. *J. Qual. Technol.* **1991**, *23*, 296–303. [CrossRef]
34. Shu, L.; Jiang, W.; Wu, S. A one-sided EWMA control chart for monitoring process means. *Commun. Stat. Simul. Comput.* **2007**, *36*, 901–920. [CrossRef]
35. Shu, L.; Jiang, W. A new EWMA chart for monitoring process dispersion. *J. Qual. Technol.* **2008**, *40*, 319–331. [CrossRef]
36. Steiner, S.H. EWMA control charts with time-varying control limits and fast initial response. *J. Qual. Technol.* **1999**, *31*, 75–86. [CrossRef]
37. Lucas, J.M.; Saccucci, M.S. Exponentially weighted moving average control schemes: Properties and enhancements. *Technometrics* **1990**, *32*, 1–12. [CrossRef]